Ultrafast carrier dynamics in a highly excited GaN epilayer

C. K. Choi, Y. H. Kwon, J. S. Krasinski,* G. H. Park, G. Setlur, and J. J. Song
Center for Laser and Photonics Research and Department of Physics, Oklahoma State University, Stillwater, Oklahoma 74078-0444

Y. C. Chang
Department of Physics and Materials Research Laboratory, University of Illinois at Urbana-Champaign, Urbana, Illinois 61801-3080
(Received 3 September 1999; revised manuscript received 7 June 2000; published 1 March 2001)

Femtosecond pump-probe transmission spectroscopy was performed at 10 K to study the nonequilibrium carrier dynamics in a GaN thin film for carrier densities ranging from 4×10^{17} to $10^{19}\,\mathrm{cm}^{-3}$. Spectral hole burning was initially peaked roughly at the excitation energy for an estimated carrier density of $4\times10^{18}\,\mathrm{cm}^{-3}$ and gradually redshifted during the excitation. Because of hot phonon effects, a very slow energy relaxation of the hot carriers at these densities was observed. The hot carriers were strongly confined in a nonthermal distribution and they relaxed collectively to the band edge for ~1 ps. We observed remarkable persistence of the excitonic resonances in GaN at carrier densities well above the Mott density at early time delays, indicating that the excitons do not strongly couple to the nonthermal electron-hole plasma.

DOI: 10.1103/PhysRevB.63.115315 PACS number(s): 78.20.−e, 78.47.+p, 71.35.Lk, 71.35.−y

Developments in femtosecond laser technology have enabled fundamental studies of nonequilibrium, nonlinear, and transport properties of semiconductors.[1] Nondegenerate pump-probe (PP) spectroscopy is a powerful tool for studying the transient dynamics of hot carriers because it makes possible the observation of not only coherent phenomena occurring during excitation, but also the nonthermal carrier distribution reflecting the energy profile of the exciting pump pulse and its temporal evolution. Wurtzite GaN has a direct band gap of 3.50 eV at 10 K, a large exciton binding energy of ~21 meV, and a large LO-phonon energy of 92 meV. Also, GaN is mechanically and thermally robust and has a higher damage threshold, making it a good candidate for investigating nonthermal carrier dynamics under strong excitation. There have been a few femtosecond PP spectroscopy reports on GaN.[2–4] However, there has been no direct experimental observation of the nonthermal carrier distributions during the pump-pulse duration and their relaxation.

We present a study of nonequilibrium carrier dynamics in a GaN epilayer photoexcited well above the band gap using nondegenerate PP spectroscopy at 10 K with light pulses of a duration time of ~360 fs at excitation densities both above and below the Mott density ($10^{18}\,\mathrm{cm}^{-3}$ for GaN at 10 K).[5] We found that the photo-excited hot carriers are strongly confined in a nonthermal distribution and their relaxation toward the band edge is very slow, partially because of the hot-phonon effect. By investigating the change of absorption spectra at the exciton resonances while the nonthermal carriers relax, we were able to evaluate the relative importance of long-range Coulomb screening and Pauli blocking on the bleaching of exciton resonances.

The sample used in this paper is a high quality 0.38 μm uncoated GaN epilayer grown by metalorganic chemical vapor deposition on (0001) sapphire. An excitonic resonance was clearly observed in this sample's absorption measurements above 300 K.[6] Femtosecond PP spectroscopy measurements were carried out using a 1 kHz regenerative amplifier (REGEN) to create 100 fs duration [full width at half maximum (FWHM)] pulses at a wavelength of 800 nm. These pulses were fed into an optical parametric amplifier to create pulses with a FWHM of 355 fs, measured by difference-frequency mixing in a BBO crystal, at 329 nm (3.766 eV) with a bandwidth of 22 meV. This beam was used as the pump source to excite carriers above the GaN band gap. The leftover output from the REGEN was frequency doubled to 400 nm and then used to create a broadband continuum probe source with a FWHM of 350 fs. The pump and probe beams were orthogonally polarized, and the angle between them was 15°. Neutral density filters were used to attenuate the probe beam to a power sufficiently low so that it would not alter the optical properties of the sample. The probe beam was focused to a 150 μm diameter spot on the sample, and the transmitted light was collected and focused into a spectrometer with an attached charge-coupled device detector. The pump spot size was focused to 300 μm to minimize the variation in the pump beam intensity across the probed region. The optical delay between the pump and the probe was accurately controlled using a computerized step motor. All measurements were performed at 10 K.

Differential transmission spectra (DTS)[7] measures the difference between the probe transmission with and without the pump

$$\mathrm{DTS}=\Delta T/T_0=(T-T_0)/T_0=\exp\left(-\int_0^d \Delta\alpha(z)\,dz\right)-1, \tag{1}$$

where T, T_0, $\Delta\alpha(z)$, and d are the transmitted probe intensity with and without the pump, the pump-induced absorption change at depth z, and the sample thickness, respectively. Figure 1 shows the DTS at early time delays for a peak carrier density of (a) $1\times10^{19}\,\mathrm{cm}^{-3}$ and (b) $4\times10^{18}\,\mathrm{cm}^{-3}$, respectively. The peak carrier densities are estimated based on theoretical modeling taking into account the band filling effect at zero time delay (see below). For the sample thickness of 0.38 μm with an absorption coefficient

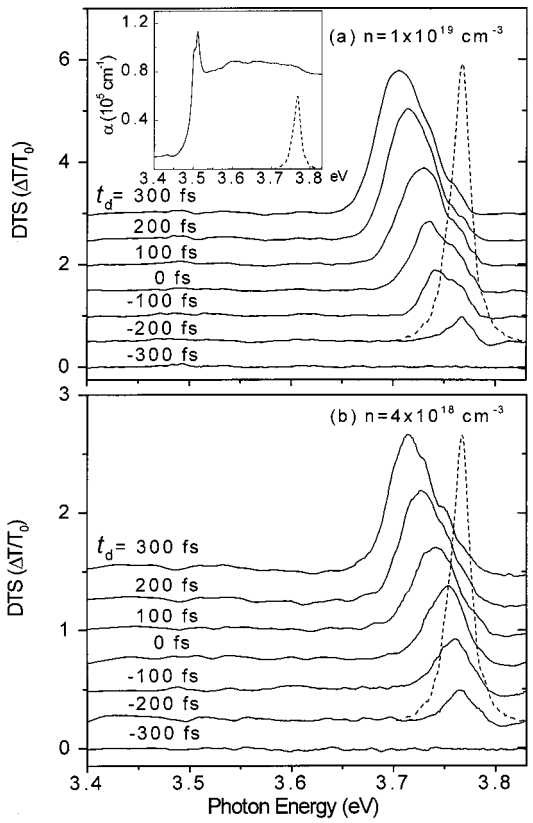

FIG. 1. Differential transmission spectra (pump-induced transmission change $\Delta T/T_0$) in a 0.38 μm GaN/sapphire sample at 10 K for peak carrier densities of (a) $1\times10^{19}\,\mathrm{cm}^{-3}$ and (b) $4\times10^{18}\,\mathrm{cm}^{-3}$ showing ultrafast near-zero-delay dynamics. The dashed line shows the pump spectra. The DTS curves were displaced vertically for clarity. The inset in Fig. 1(a) shows the absorption spectra for the sample at 10 K.

of $0.8\times10^5\,\mathrm{cm}^{-1}$ at the excitation energy, our sample is optically thick, so the carrier density depends on the depth (z) from the sample surface, which leads to a depth-dependent absorption coefficient $\alpha(z)$. The pump spectrum is shown as a dashed line and centered at 3.766 eV (266 meV above the band gap of the excited GaN sample at 10 K). The inset in Fig. 1(a) shows well-resolved 1s A- and B-exciton resonances. The DTS value, which is larger than unity, does not indicate optical gain, but rather a large induced transparency by the strong laser excitation. Due to strong band filling effects, there is a large reduction of about $10^4\,\mathrm{cm}^{-1}$ in absorption of the probe intensity. This makes T an order of magnitude larger than T_0, leading to a DTS value larger than one. We take the zero time delay to be at the approximate maximum of the pump pulse. For time delays of less than -200 fs, there were no significant band filling effects, which is characteristic of an unexcited sample. Coherent oscillation effects[8] around exciton resonances and in the vicinity of the excitation energy when the probe pulse precedes the pump were not observed in our experiment.

The DTS at a time delay of $t_d=-200$ fs shows a spectral hole burning[9] that is initially peaked roughly at the excitation energy. While the population of excited carriers increases during the pump duration (from -200 to 200 fs), the spectral hole burning shows fast broadening and distinct shifts of 47 meV [Fig. 1(a)] and 38 meV [Fig. 1(b)] toward the band gap. The fast broadening of the nonequilibrium carrier distribution at this time scale is most likely caused by carrier-carrier scattering, such as electron-electron, electron-hole, and hole-hole collisions. Because the initial excess electron energy is about three times larger than the hole energy and because of the larger electron-to-hole effective mass ratio in GaN compared to GaAs, the transfer of energy to the colder hole system via electron-hole scattering could result in this fast broadening of the hole burning. The redshift of the spectral hole on this time scale of less than 200 fs cannot be ascribed to a relaxation of the carrier distribution through LO-phonon emission, because the redshift is much smaller than the LO-phonon energy of 92 meV, and the deformation-potential scattering is not strong enough to cause such a redshift at an early time delay. We neglect the carrier diffusion effect, because the diffusion constant for a GaN/AlGaN double heterostructure within 2 ps at 10 K was reported to be small.[10]

To investigate the carrier dynamics, we adopt a simplified model that takes into account the carrier-carrier scattering with static screening and various electron-phonon scattering processes. We have considered the electron-phonon scattering by both the Fröhlich and the deformation-potential mechanisms. We found that at a peak carrier density of $n=4\times10^{18}\,\mathrm{cm}^{-3}$, for energies near the pumping energy, the carrier-carrier scattering rate is around 80 (460) ps^{-1} for electrons (holes), while the electron-LO phonon scattering rate is around 60 ps^{-1}. The hole-LO scattering rate is negligible, since the hole energies are smaller than the LO-phonon energy and therefore, no LO-phonon emission process is possible. At $n=1\times10^{19}\,\mathrm{cm}^{-3}$, these rates change to 50 (300) ps^{-1} and 50 ps^{-1}, respectively. Thus, both mechanisms are important for the energy relaxation of carriers. The screening effect reduces both the carrier-carrier scattering and electron-LO phonon scattering, but not substantially. Without carrier screening, the electron-LO phonon scattering rate is around 80 ps^{-1}, which is consistent with the result reported in Ref. 11. Since the electron-LO phonon scattering rate is much higher than the decay rate of LO phonons (around 0.2 ps^{-1})[12] even at the highest density considered here, we expect that a large number of nonequilibrium (hot) LO phonons is generated during the carrier relaxation. It is well known that the presence of hot phonons substantially reduces the energy relaxation rate of electrons,[13–15] since the equivalent temperatures of the hot electrons and hot phonons are close to each other. Thus, it is not surprising that our electron energy relaxation is slow (around 100 meV/ps). In this paper, we concentrate on the simulation of the PP spectra at early times during the carrier buildup. For a time delay less than 100 fs, the carrier distribution remains peaked at the same position in momentum space, with a gradual broadening due to the carrier-carrier scattering.

The nonlinear transmission change cannot be readily interpreted in terms of band filling alone. The complex superposition of band-gap renormalization, band filling, and the screening of the Coulomb interaction between correlated-states (excitons) and uncorrelated electron-hole pairs must be

taken into account.[16] We attribute the spectral hole redshift at early times to band-gap renormalization and exciton effects. A weak induced absorption at $t_d=-200$ fs in Figs. 1(a) and 1(b) is seen just above the excitation energy. This could be due to Coulomb enhancement by exciton effects. The induced absorption disappears with increasing carrier density when electron-hole plasma screening of the Coulomb potential overwhelms the attractive electron-hole interaction. There have been a few reports on induced absorption above the excitation energy for GaAs.[17,18] They attributed the induced absorption to a many-body correlation from Coulomb interaction. In general, exciton effects result in a small redshift of the spectral hole to lower energies.[16–19] However, this effect alone does not explain our result, since the spectral hole moves toward the band edge during the pump duration, contrary to what is observed in GaAs.[17] We consider the momentum (k) dependence of the band-gap renormalization $\Delta E(k)$, taking into account the actual carrier distribution. The k dependence of the band-gap renormalization is calculated first in the Hartree-Fock approximation and then with the addition of the Coulomb-hole effect.[20] We then have

$$\Delta E(k)=-\Sigma_q v_q f(k+q)/\epsilon(q)-\Sigma_q v_q[\epsilon(q)^{-1}-\epsilon_0^{-1}], \tag{2}$$

where $v_q=4\pi e^2/q^2$, ϵ_0 is the low-frequency dielectric constant, $\epsilon(q)$ is the static dielectric function including the polarization due to free carriers, and $f(k)$ is the nonequilibrium carrier distribution function. The first term is the screened Hartree-Fock approximation and the second term is the Coulomb-hole correction. The dielectric screening in the static limit is approximately given by Lindhard's expression

$$\epsilon(q)=\epsilon_0+2v_q\Sigma_k\frac{f(k)-f(k+q)}{E(k+q)-E(k)}$$

$$=\epsilon_0+\frac{2e^2m^*}{\hbar^2\pi q^3}\int \ln\left|\frac{q+2k}{q-2k}\right|[f(k)(k)(dk)], \tag{3}$$

where, in the long-wavelength limit, we have

$$\epsilon(q)=\epsilon_0(1+{q_0}^2/q^2) \quad \text{with}$$

$$q_0^2=(2e^2m^*/\hbar^2\pi\epsilon_0)\left[\int f(k)(dk)\right]. \tag{4}$$

Note that q_0 reduces to the Thomas-Fermi wave vector in the degenerate limit when $f(k)$ becomes the Fermi distribution function at zero temperature.

We found that the nonequilibrium carrier distributions can be approximated by the Gaussian distribution

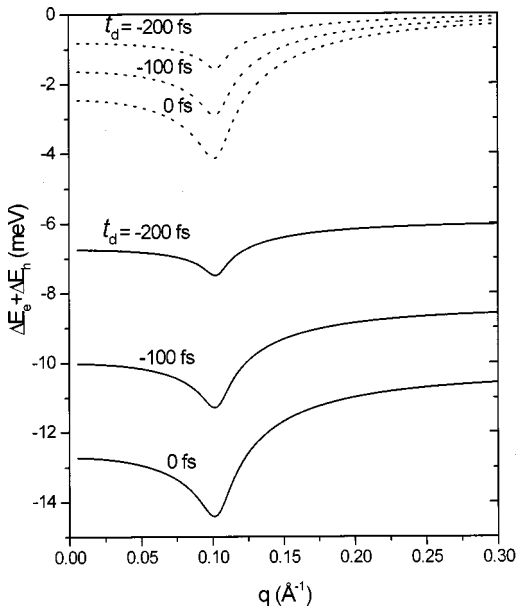

FIG. 2. Calculated band renormalization for the A band transition due to nonequilibrium carrier distribution as a function of momentum at a depth $z=d/4$ for a peak carrier density of $4\times10^{18}\,\mathrm{cm}^{-3}$, at time delays of $t_d=-200$, -100, and 0 fs. The dotted lines represent the screened Hartree-Fock approximation. The solid lines also include the Coulomb-hole correction.

$$f_e(k)=A(z)[\exp\{-a(k^2-k_1^2)^2\}+\exp\{-a(k^2-k_2^2)^2\}], \tag{5}$$

$$f_{h1}(k)=A(z)[\exp\{-a(k^2-k_1^2)^2\}], \tag{6}$$

$$f_{h2}(k)=A(z)[\exp\{-a(k^2-k_2^2)^2\}], \tag{7}$$

where the subscripts e, $h1$, and $h2$ label the electrons, holes in the A band, and holes in the B band, respectively. The amplitude of the carrier distribution is assumed to be proportional to the light intensity at depth z. Thus, we have the following form $A(z)=A_0e^{-\alpha z}$, where α is the absorption coefficient at the pump energy. The peak carrier density that we used throughout this paper is given by $n=2\int f_e(k)dk/(2\pi)^3$ at a depth of $z=0$. The centering positions k_1 and k_2 are determined by the relation

$$E_e(k_1)+E_{h1}(k_1)=E_e(k_2)+E_{h2}(k_2)=\hbar\omega, \tag{8}$$

where $\hbar\omega$ is the absorbed photon energy. For illustration, we show in Fig. 2 the k-dependent band renormalization for the A-band transitions for a carrier density $n(z)=(4\times10^{18}\,\mathrm{cm}^{-3})e^{-\alpha z}$ with the depth set at $z=d/4$. The band renormalization for the B-band transitions is quite similar to that of the A-band transitions. Using the z-dependent band renormalization and nonequilibrium carrier distributions given above, we calculated the z-dependent absorption coefficient $\alpha(z)$ and DTS according to Eq. (1). The absorption coefficient for the A-band transitions, including phase-space filling and neglecting screening, is given by

$$\alpha(\hbar\omega)=(C/\hbar\omega)\Big[\delta(\hbar\omega-E_g-E_X)+\delta(\hbar\omega-E_g-E_X/4)/8$$
$$+\frac{2\pi^2 x}{1-e^{-2x}}\Sigma_k\{[1-f_e(k)-f_h(k)]\delta[\hbar\omega-E_e(k)$$
$$-E_h(k)-\Delta E_e(k)-\Delta E_h(k)]\}, \quad (9)$$

where C is a constant, E_g is the energy gap between the renormalized valence band (A or B band) and the conduction band, E_X is the exciton binding energy, $x=[E_X/(\hbar\omega-E_g)]^{1/2}$. The z dependence for $f_e(k)$, $f_h(k)$, ΔE_e, ΔE_h, and α was kept implicit in the above equation. The absorption coefficient for the B-band transitions is given by the same expression, except that the band gap E_g is increased by the A-B splitting and the constant C is increased by 20% in order to reproduce the line shape of the experimental spectrum near the exciton energy. Note that we included the contributions from the ground state, the first excited state, and the continuum states (with the phase-space filling effect). In our initial simulation, due to band renormalization, an appreciable DTS occurs near the exciton energy, in disagreement with our experiment. However, the DTS predicted near the pump energy is in reasonable agreement with experiment. This suggests that the band renormalization in the correlated exciton states is greatly suppressed due to the charge neutrality of the exciton. Since a full many-body theory is not available at the present, we introduce a phenomenological suppressing factor $\{1-\exp[-(E_e(k)+E_h(k)-E_g)/4E_X]\}$. This factor greatly reduces the band renormalization for the exciton continuum states with low energy, while the high-energy states are unaffected. This is reasonable, since the high-energy exciton continuum states are much less correlated. With this correction, the final simulated absorption spectra averaged over the sample depth, $[\int_0^d \alpha(z)dz]/d$, and the DTS are shown in Fig. 3, and are seen to be in reasonable agreement with experiment. For comparison, the DTS at $t_d=0$ fs without including the correction factor is shown as the short dotted curve, and is in poor agreement with experiment near the exciton transition energy.

In contrast to GaAs, intervalley scattering does not occur in GaN for an excitation energy of 3.766 eV,[4] so electrons excited from the three valence bands into the conduction band reside in the Γ valley for all time delays. Compared to the rapid hot carrier redistribution in GaAs (Ref. 21) and CdSe (Ref. 22) over a wide energy range within 100 fs at much lower excitation density, Fig. 4(a) shows that the hot carriers in GaN relax extremely slowly toward the band edge and are strongly restrained in a nonthermal distribution for $\sim$1 ps, as shown by their rather narrow spectral peak. No LO phonon replica is observed for $t_d \leqslant 0.7$ ps, indicating a strong suppression of electron-LO phonon interaction. The detailed mechanism for this suppression remains unclear. One possible mechanism involves the anisotropy factor $(L_{kk'})$, which appears in the coupling matrix element and is proportional to the overlap of Bloch states of different wave

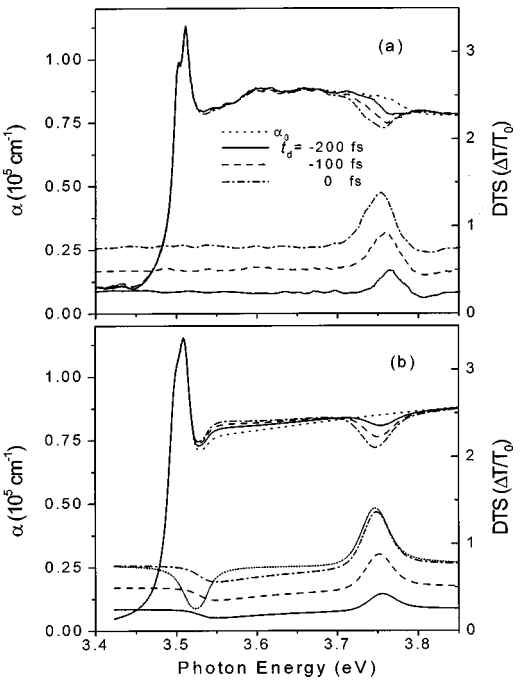

FIG. 3. (a) Measured absorption and DTS at time delays of $t_d=-200$, -100, and 0 fs and at a peak carrier density of $4\times10^{18}\,\mathrm{cm}^{-3}$. The dotted α_0 lines are the values taken without the pump beam. (b) The same as (a), except theoretically calculated (see text). The DTS curves are displaced vertically for clarity in both cases.

vectors. This factor could be much less than 1 if the difference between k and k' is large. Assuming that electron-LO phonon scattering is blocked at early time delays, we can get insight into the role of carrier-carrier (CC) interaction in the initial thermalization through a comparison of our experimental results with a previous study of PP spectroscopy on bulk GaAs at 15 K, in which the carriers were excited well above the band gap similarly to our experimental conditions.[23] At a carrier density of $7\times10^{17}\,\mathrm{cm}^{-3}$, the GaAs showed that the effective energy exchange among the carriers leads to an ultrafast thermalization by about 100 fs. At a high peak carrier density of $4\times10^{18}\,\mathrm{cm}^{-3}$ in GaN, our simulation results using screened CC interactions alone showed that the CC scattering already leads to a Fermi-Dirac distribution for the hot carriers (with a temperature consistent with the total kinetic energy of the carriers) at $t_d=\sim0.5$ ps. Including the electron-LO phonon scattering clearly produces a LO phonon replica at 92 meV below the initial peak. This is inconsistent with our experimental result, which shows a nonthermal carrier distribution up to $\sim$1 ps. This experiment suggests that there are other mechanisms that block the electron-LO phonon interaction and impede the carrier-carrier scattering. The mechanisms for such a surprisingly slow thermalization process is still unclear.

We were able to clearly observe LO-phonon emission processes at time delays from 0.7 to 1.3 ps with a peak carrier density of $1\times10^{19}\,\mathrm{cm}^{-3}$, as shown in Fig. 4(a). At $t_d=0.9$ ps, a shoulder arises at 3.56 eV because of the emission of single LO phonons from the electron-hole plasma,

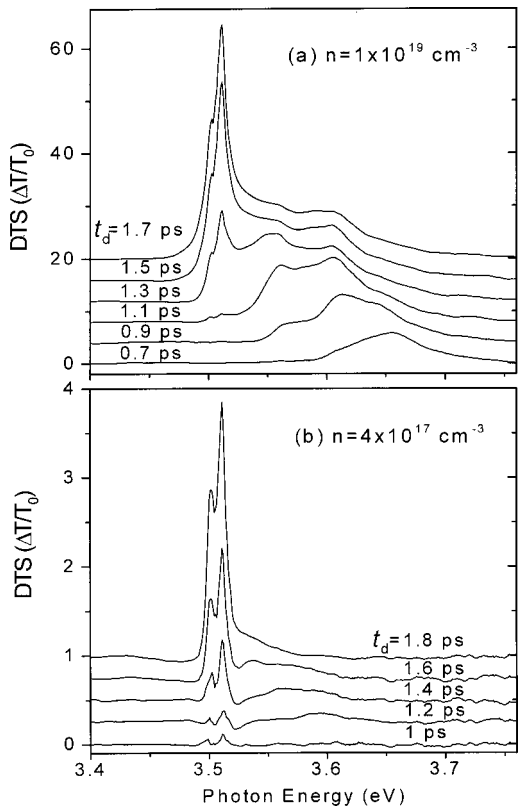

FIG. 4. Spectrally resolved transmission changes as a function of time delay at peak carrier densities of (a) $1\times10^{19}\,\mathrm{cm}^{-3}$ and (b) $4\times10^{17}\,\mathrm{cm}^{-3}$. The spectra were recorded 200 fs apart and displaced vertically for clarity.

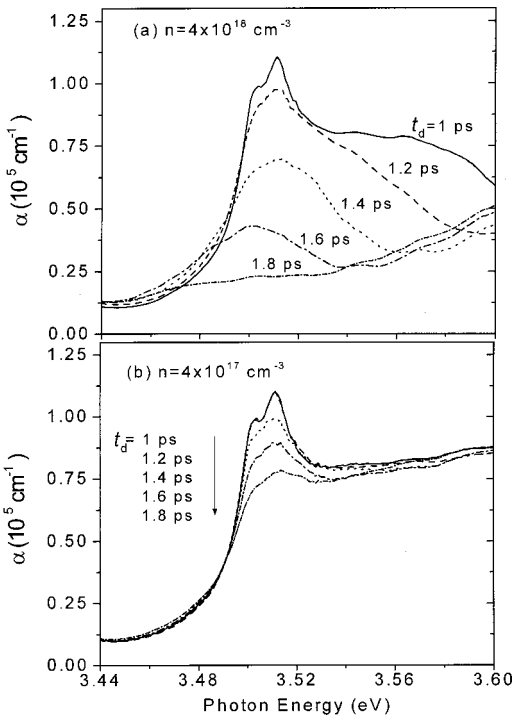

FIG. 5. Absorption spectra near the band edge of GaN as a function of time delay for peak carrier densities of (a) $4\times10^{18}\,\mathrm{cm}^{-3}$ and (b) $4\times10^{17}\,\mathrm{cm}^{-3}$. The spectra were recorded at 200 fs intervals from 1 to 1.8 ps. Note the induced absorption below the band edge.

which is peaked at 3.65 eV at $t_d=0.7\,\mathrm{ps}$. With continuing LO-phonon emissions via the screened Fröhlich interactions, the shoulder grows and redshifts with increasing time delay. It is worth noting that the nonthermal carrier distribution at $t_d=1.1\,\mathrm{ps}$ in Fig. 4(a), which appears as two separate peaks as a result of the LO-phonon emission, does not disappear very quickly. This indicates strong competition between the LO-phonon scattering process (including both emission and absorption) and the carrier-carrier scattering process, since they have comparable rates. At a peak carrier density of $4\times10^{17}\,\mathrm{cm}^{-3}$, the carrier relaxation is almost completed at $t_d=1.8\,\mathrm{ps}$, as shown in Fig. 4(b). However, at a peak carrier density of $1\times10^{19}\,\mathrm{cm}^{-3}$, many hot carriers are located at 3.60 eV at $t_d=1.7\,\mathrm{ps}$, which means that the hot phonon effects are evident at high carrier density.

The presence of electrons and holes reduces the effective electron-hole attraction, not only through screening, but also through Pauli blocking (phase-space filling and short-range exchange effects). Both effects are always simultaneously present, but their relative importance changes with the dimensionality of the system.[24] Figure 5 shows absorption spectra near the band edge of GaN as a function of time delay at carrier densities both (a) above and (b) below the Mott density. Below the Mott density, as shown in Fig. 5(b), exciton resonances saturate in a way that maintains the peak energy position through a balance between the reduction of the exciton binding energy and a redshift produced by the band-gap renormalization.[25] On the other hand, at a peak carrier density of $4\times10^{18}\,\mathrm{cm}^{-3}$ (higher than the Mott density), a redshift of 10 meV at $t_d=1.6\,\mathrm{ps}$ is seen in Fig. 5(a), indicating that the redshift produced by the band-gap renormalization dominates over the reduction of the exciton binding energy. Using the long-wavelength approximation $[\epsilon(q)=\epsilon_0(1+q_0^2/q^2)]$ in Eq. (4), we estimate the long-range Coulomb screening effects by the nonthermal carriers on the exciton resonances. The screening length (q_0) at a peak carrier density of $4\times10^{18}\,\mathrm{cm}^{-3}$ decreases by only a factor of two from 200 to 1.8 ps. Further, we could not observe appreciable exciton bleaching effects, until 1 ps when the carriers began to fill the near-band-edge states, indicating that long-range Coulomb screening by the nonequilibrium carriers does not provide the main contribution to the exciton bleaching. This could originate from the fact that the excitons do not strongly couple to nonthermal electron-hole plasma owing to overall charge neutrality. Similar delayed exciton bleaching was also observed in CuCl.[26]

In conclusion, we studied the hot carrier dynamics in a GaN epilayer excited well above the band edge at 10 K under high-carrier densities. A spectral hole was initially peaked roughly at the excitation energy and gradually redshifted during the pump duration. We attributed the redshift of the hole to a combination of exciton effects and band-gap renormalization, which takes into account the nonequilibrium carrier distribution. Energy relaxation and thermaliza-

tion of the hot carriers are extremely slow, due to blocking of the electron-LO phonon interaction and a large reduction in carrier-carrier scattering. At about 900 fs, LO-phonon emission processes via the screened Fröhlich mechanism were clearly observed at a peak carrier density of $1\times10^{19}\,\mathrm{cm}^{-3}$. We found that phase-space filling and short-range exchange effects based on the Pauli exclusion principle play a more important role in the exciton bleaching than long-range Coulomb screening.

This work was supported by BMDO, AFOSR, ONR, and NSF.

*Center for Laser and Photonics Research and Department of Electrical Engineering and Computer Science, Oklahoma State University, Stillwater, Oklahoma 74078.

[1] For an overview, see, for example, J. Shah, *Ultrafast Spectroscopy of Semiconductors and Semiconductor Nanostructures* (Springer-Verlag, Berlin, 1996).
[2] S. Hess, F. Walraet, R. A. Taylor, J. F. Ryan, B. Beaumont, and P. Gibart, Phys. Rev. B **58**, 15 973 (1998).
[3] Hong Ye, G. W. Wicks, and P. M. Fauchet, Appl. Phys. Lett. **74**, 711 (1999).
[4] C.-K. Sun, Y.-L. Huang, S. Keller, U. K. Mishra, and S. P. DenBaars, Phys. Rev. B **59**, 13 535 (1999).
[5] F. Binet, J. Y. Duboz, J. Off, and F. Scholz, Phys. Rev. B **60**, 4715 (1999).
[6] A. J. Fischer, W. Shan, J. J. Song, Y. C. Chang, R. Horning, and B. Goldenberg, Appl. Phys. Lett. **71**, 1981 (1997).
[7] N. Peyghambarian, S. W. Koch, and A. Mysyrowicz, *Introduction to Semiconductor Optics* (Prentice-Hall, New Jersey, 1993), p. 384.
[8] B. Fluegel, N. Peyghambarian, G. Olbright, M. Lindberg, S. W. Koch, M. Joffre, D. Hulin, A. Migus, and A. Antonetti, Phys. Rev. Lett. **59**, 2588 (1987).
[9] J. L. Oudar, D. Hulin, A. Migus, A. Antonetti, and F. Alexandre, Phys. Rev. Lett. **55**, 2074 (1985).
[10] W. Shan, S. Xu, B. D. Little, X. C. Xie, J. J. Song, G. E. Bulman, H. S. Hong, M. T. Leonard, and S. Krishnankutty, J. Appl. Phys. **82**, 3158 (1997).
[11] C. Y. Tsai, C. H. Chen, T. L. Sung, C. Y. Tsai, and J. M. Rorison, J. Appl. Phys. **85**, 1475 (1999).
[12] K. T. Tsen, R. P. Joshi, D. K. Ferry, A. Botchkarev, B. Sverdlov, A. Salvador, and H. Morkoc, Appl. Phys. Lett. **68**, 2990 (1996).
[13] J. Shah, A. Pinczuk, A. C. Gossard, and W. Wiegmann, Phys. Rev. Lett. **54**, 2045 (1985).
[14] P. Lugli, Solid-State Electron. **31**, 667 (1988).
[15] D. S. Kim and P. Y. Yu, Phys. Rev. B **43**, 4158 (1991).
[16] J. Nunnenkamp, J. H. Collet, J. Klebniczki, J. Kuhl, and K. Ploog, Phys. Rev. B **43**, 14 047 (1991).
[17] J.-P. Foing, D. Hulin, M. Joffre, M. K. Jackson, J.-L. Oudar, C. Tanguy, and M. Combescot, Phys. Rev. Lett. **68**, 110 (1992).
[18] C. Fürst, A. Leitenstorfer, A. Laubereau, and R. Zimmermann, Phys. Rev. Lett. **78**, 3733 (1997).
[19] S. Hunsche, H. Heesel, A. Ewertz, H. Kurz, and J. H. Collet, Phys. Rev. B **48**, 17 818 (1993).
[20] G. B. Ren and P. Blood, Phys. Rev. B **60**, 16 675 (1999).
[21] T. Elsaesser, J. Shah, L. Rota, and P. Lugli, Phys. Rev. Lett. **66**, 1757 (1991).
[22] B. D. Fluegel, A. Paul, K. Meissner, R. Binder, S. W. Koch, N. Peyghambarian, F. Sasaki, T. Mishina, and Y. Masumoto, Solid State Commun. **83**, 17 (1992).
[23] A. Alexandrou, V. Berger, D. Hulin, and V. Thierry-Mieg, Phys. Status Solidi B **188**, 335 (1995).
[24] T. Ando, A. B. Fowler, and F. Stern, Rev. Mod. Phys. **54**, 437 (1982).
[25] R. Zimmermann, Phys. Status Solidi B **146**, 371 (1988).
[26] A. Antonetti, D. Hulin, A. Migus, A. Mysyrowicz, and L. L. Chase, J. Opt. Soc. Am. B **2**, 1197 (1985).